

Contents lists available at ScienceDirect

Science Bulletin

journal homepage: www.elsevier.com/locate/scib



Short Communication

Boosting zinc anode durability through synergistic inner Helmholtz plane and interfacial electric field regulation

Hao Tan a, Chao Meng a, Tong Sun b, Xing-Long Wu c,*, Hong Liu a,d,*, Jian-Jun Wang a,e,*

- ^a State Key Laboratory of Crystal Materials, Shandong University, Jinan 250100, China
- ^b College of Chemistry and Chemical Engineering, Qingdao University, Qingdao 266071, China
- CMOE Key Laboratory for UV Light-Emitting Materials and Technology, Department of Physics, Northeast Normal University, Changchun 130024, China
- ^d Jinan Institute of Quantum Technology, Jinan Branch, Hefei National Laboratory, Jinan 250101, China
- e Shenzhen Research Institute, Shandong University, Shenzhen 518057, China

ARTICLE INFO

Article history:
Received 8 February 2024
Received in revised form 1 April 2024
Accepted 22 April 2024
Available online 26 April 2024

© 2024 Science China Press. Published by Elsevier B.V. and Science China Press. All rights are reserved, including those for text and data mining, Al training, and similar technologies.

As the need for energy storage devices escalates, aqueous zincion batteries (ZIBs) have risen as a promising alternative to the widely used Li-ion batteries, offering intrinsic safety, environmental compatibility, and cost advantages, positioning them as attractive energy storage systems for the future [1,2]. However, challenges such as dendrite growth on Zn anodes, stemming from uneven electric fields on the surface and active water side reactions, compromise cycling stability and lifespan, posing significant hurdles for the practical application of ZIBs [3,4]. To mitigate these issues, strategies like electrolyte optimization, artificial solid electrolyte interphase (SEI) layers, and current collector modifications have been proposed [5,6]. Nevertheless, most long-cycle experiments are conducted at low current densities and deposition capacities, with high current density and capacity operations typically lasting less than 1000 h [7].

Interfacial chemistry plays a crucial role in regulating the Zn deposition process [8]. The SEI layer, often formed by electrolyte additives or artificial constructs, is vital in preventing direct zincelectrolyte contact, yet challenges persist regarding ion conductivity and mechanical strength [9,10]. In the absence of an SEI layer, the electric double layer (EDL), comprising the Helmholtz layer and diffusion layer, becomes critical in regulating interfacial reactions [11–13]. The inner Helmholtz plane (IHP) within the Helmholtz layer dictates the de-solvation, diffusion, and electrochemical deposition of Zn²⁺ ions. For instance, in a pure ZnSO₄ electrolyte, the IHP is formed by SO₄²⁻ anions and water dipoles, with de-solvation occurring at the outer Helmholtz plane-IHP interface [14]. This leads to significant hydrogen evolu-

E-mail addresses: xinglong@nenu.edu.cn (X.-L. Wu), hongliu@sdu.edu.cn (H. Liu), wangjianjun@sdu.edu.cn (J.-J. Wang).

tion reactions (HER) and zinc corrosion due to the low redox potential. Additionally, the high de-solvation energy of $Zn(H_2O)_6^{2+}$ in the outer Helmholtz plane causes local polarization, increasing the risk of HER in the IHP [15]. Although the IHP significantly influences battery performance, its complexity makes it difficult to manipulate for enhanced interfacial stability. The EDL structure also critically affects the electric field distribution at the interface, influencing the Zn²⁺ deposition on the zinc anode [16]. The "tip effect" exacerbates uneven electric fields, promoting dendrite growth and perpetuating a cycle of surface roughness [17]. Therefore, simultaneously controlling the IHP structure and surface electric field is vital to suppress dendrite growth and reduce side reactions but remains a considerable challenge. Herein, we introduce 1-ethyl-3-methylimidazolium acetate (EMImOAc) as an innovative additive to concurrently regulate the molecular distribution within the IHP and the Zn²⁺ solvation sheath and fine-tune the surface electric field, resulting in water-depleted IHP to mitigate water splitting and homogenized surface electric field to thereby ameliorate Zn²⁺ ion concentration polarization, culminating in exceptional stability.

The interaction between $\rm ZnSO_4$ and EMImOAc in the electrolyte was initially probed by examining the $\rm Zn^{2^+}$ solvation sheath and the hydrogen bond network. A blue shift in the O—H stretching vibration from 3223 cm⁻¹ in 2 mol L⁻¹ ZnSO₄ to 3230 cm⁻¹ corroborates the disruption of the H-bond network upon EMImOAc addition (Fig. 1a). Furthermore, the addition of EMImOAc led to a downfield shift in the 2 H nuclear magnetic resonance (NMR) signal from 4.75 ppm in 2 mol L⁻¹ ZnSO₄ to 4.78 ppm, indicative of an increased de-shielding effect (Fig. 1b). This shift is attributable to the formation of stronger H-bonds between anions and water molecules compared with those between water molecules alone, weakening the nuclear shielding effect on surrounding electrons.

^{*} Corresponding authors.

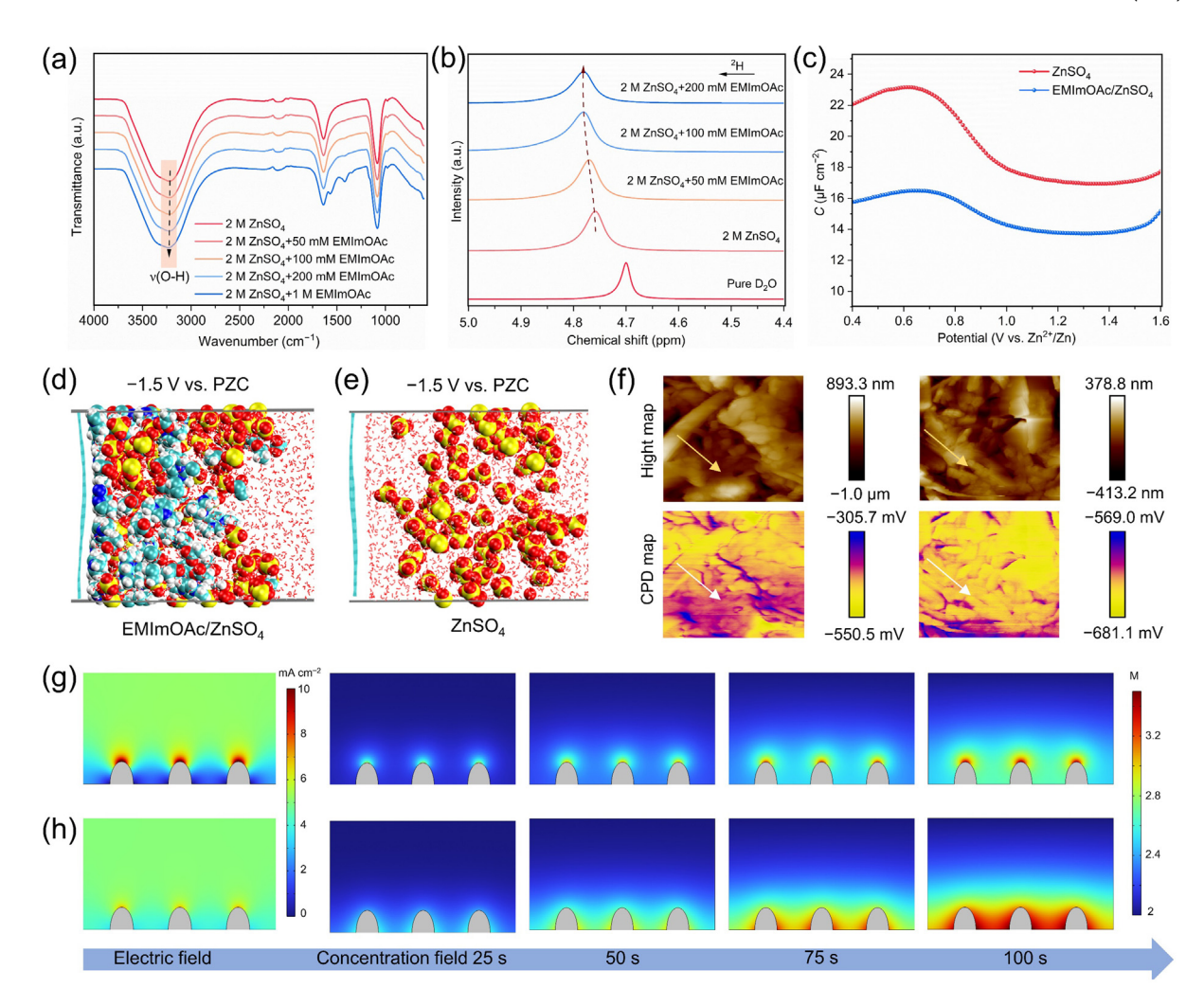


Fig. 1. (Color online) (a) Fourier transform infrared spectroscopy (FT-IR) spectra of different electrolytes (M refers to mol L⁻¹). (b) ²H NMR spectra with various concentrations of EMImOAc. (c) Differential capacitance curves recorded in different electrolytes. Snapshots of the simulated structures including (d) EMImOAc/ZnSO₄ and (e) ZnSO₄ system under -1.5 V vs. PZC. (f) AFM and KPFM images for the Zn deposition layer on Cu foils in ZnSO₄ (left) and EMImOAc/ZnSO₄ (right) electrolytes. The scan size is 5 μ m × 5 μ m. Electric field and concentration field simulation in (g) ZnSO₄ and (h) EMImOAc/ZnSO₄ electrolytes.

Furthermore, the Raman spectra suggest that EMImOAc effectively disrupts the hydrogen bonding network among water molecules (Fig. S1a and b online).

Molecular dynamics simulations provided insight into the solvation structure of Zn²⁺ ions and their radial distribution functions (RDFs) and coordination numbers in both EMImOAc/ZnSO4 and ZnSO₄ electrolytes (Fig. S1c and d online). The RDFs showed a pronounced peak at 1.92 Å with a coordination number of 4.208, corresponding to the Zn²⁺-water oxygen distance in the ZnSO₄ electrolyte. The coordination peak of Zn²⁺ with sulfate oxygen was observed at 1.8 Å with a coordination number of 1.792 (Fig. S1e online). In the presence of EMImOAc, these peaks shifted slightly to 1.92 and 1.82 Å, with coordination numbers of 4.109 and 1.836, respectively (Fig. S1f and g online). A new coordination peak emerged at 1.8 Å with a coordination number of 0.054 for Zn²⁺ with acetate oxygen (Fig. S1h online), indicating a reduction in the number of water molecules in the Zn²⁺ solvation sheath due to the presence of acetate, thereby elevating the energy barrier for HER. This alteration in the solvation structure was further substantiated by the Gibbs free energy calculations for the desolvation processes, which showed significantly higher desolvation energies of -637.6 kcal mol⁻¹ for Zn(H₂O)₄(OAc)⁺ than $-803.9 \text{ kcal mol}^{-1} \text{ for } Zn(H_2O)_4(SO_4) \text{ (Fig. S2 online)}.$

To further explore the variations within the EDL, we assessed differential capacitance as depicted in Fig. 1c. The observed reduction in capacitance upon the addition of EMImOAc can be ascribed to the pronounced adsorption of voluminous EMIm⁺ cations on the Zn surface, which consequently increases the EDL thickness. This phenomenon is further corroborated by Zeta potential measurements, density functional theory and contact angle measurements (Fig. S3a-c online). Delving deeper into the structural transformation of the IHP, we investigated the effect of applied potential on the IHP regions at the anode surface using one nano-second molecular dynamics simulations with a graphene electrode as a model system. Fig. 1d reveals that, upon increasing the potential from the potential of zero charge (PZC) to -1.5 V, EMIm⁺ cations are preferentially adsorbed and enriched on the electrode surface, displacing active water molecules from the IHP. Fig. S3d (online) graphically depicts the displacement of active water molecules by bulky EMIm⁺ cations, leading to a marked reduction in the spatial density of water at the interface, which is anticipated to bolster electrode stability. In contrast, the ZnSO₄ electrolyte system without EMIm+ shows a persistent enrichment of water molecules in the IHP, resulting in severe side reactions at the interface (Fig. 1e). Encouragingly, even with a polarization voltage of +1.5 V vs. PZC, EMIm⁺ remains predominantly within the IHP,

effectively diminishing the presence of water molecules (Fig. S3e–g online). These simulation outcomes validate that the introduction of EMIm⁺ cations fosters an IHP structure deficient in water at the interface, creating a protective barrier that prevents continuous decomposition under polarization.

Atomic force microscopy (AFM) and Kelvin probe force microscopy (KPFM) were utilized to analyze the surface topography and potential of Zn/Cu electrodes post-cycling in distinct electrolytes (Fig. 1f). AFM data indicate that the Cu foil cycled with EMImOAc/ZnSO₄ electrolyte showcases a smoother surface with an average height of 792 nm and a reduced surface potential of 122.1 mV (Fig. S4a online). In stark contrast, cycling in pure ZnSO₄ electrolyte results in an increased average height of 1.9 µm and a heightened surface potential of 344.8 mV. The detailed height and contact potential difference (CPD) profiles demonstrate a direct correlation between deposition morphology and the surface electric field (Fig. S4b and c online). Pronounced CPD fluctuations at the peaks and troughs of the deposits highlight how irregular deposition patterns exacerbate the uneven distribution of the local electric field, fostering dendritic growth from the surface tips. However, with the addition of EMImOAc, the surface height and potential distribution become significantly more uniform, suggesting that the preferential adsorption of EMImOAc effectively modulates the electric field.

Finite element modeling simulations substantiated the electrostatic shielding impact imparted by the adsorption of EMIm⁺ ions on the zinc surface. The current density and Zn²⁺ ion distribution during the deposition process reveal a notable difference between electrolytes (Fig. 1g and h). In the pure ZnSO₄ electrolyte, the current density is markedly elevated at the zinc dendrite tips, denoting an irregular local electric field that tends to concentrate at the surface irregularities. Conversely, the distribution of the electric field in the EMImOAc/ZnSO₄ electrolyte is considerably more even, attributed to the π - π conjugated EMIm⁺ cations within the IHP forming a relatively positive electrostatic layer. This layer facilitates a balanced Zn²⁺ ion distribution at the interface, resulting in a more uniform current density across the surface. To further elucidate this phenomenon, simulations of the Zn²⁺ concentration field during deposition were conducted. These simulations revealed a significant accumulation of Zn²⁺ ions at the protrusion tips while the adjacent flat regions exhibited a markedly lower Zn²⁺ concentration in the ZnSO₄ electrolyte, exacerbating dendritic growth. In contrast, the EMImOAc/ZnSO₄ electrolyte demonstrated a notably uniform Zn²⁺ concentration across the electrode surface. Notably, at a simulated diffusion time of 100 s, a pronounced disparity in concentration distribution on the surface emerged. This can be ascribed to the potent electrostatic shielding effect of EMIm⁺ ion clusters at the tips of zinc protrusions, which effectively

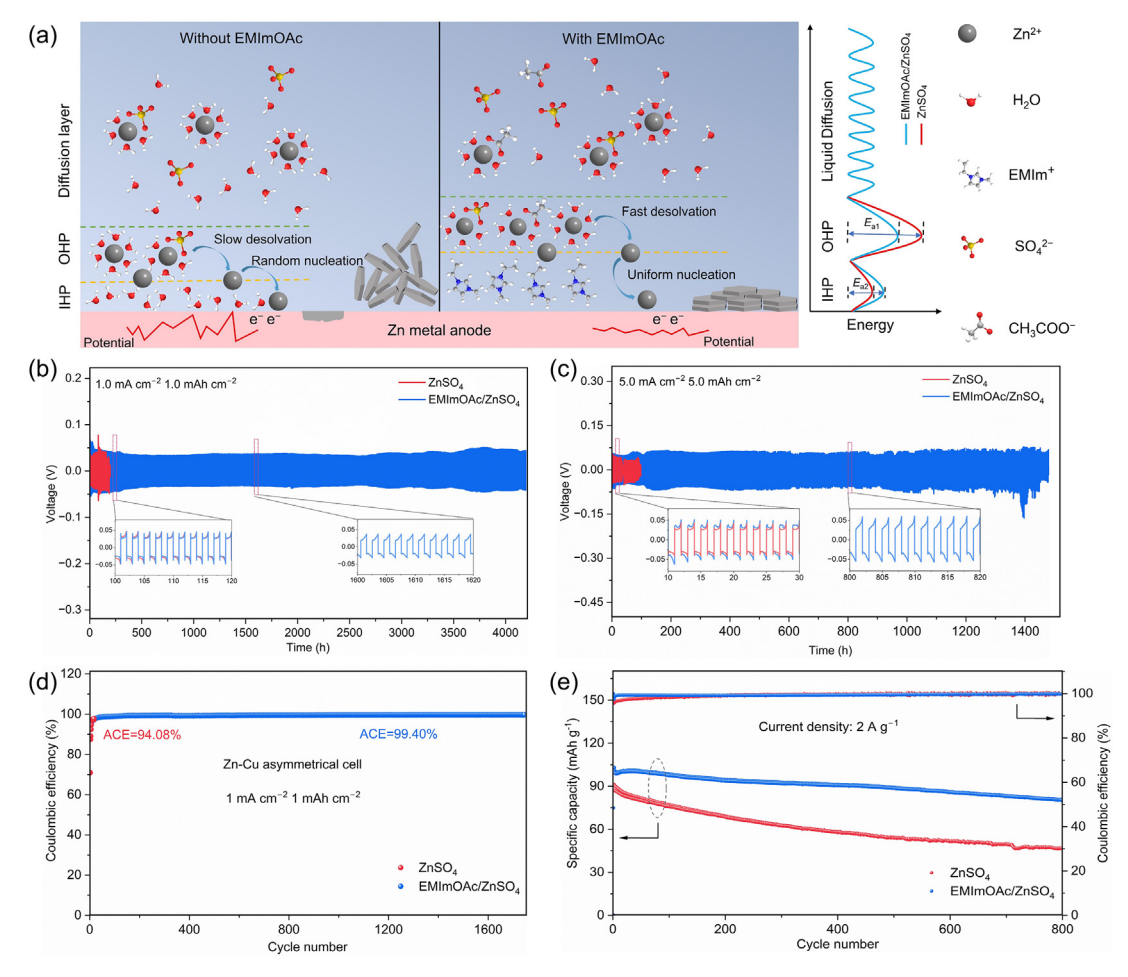


Fig. 2. (Color online) (a) Illustration of the EDL structure for Zn anodes in different electrolytes with enhanced Zn²⁺ interfacial de-solvation/transfer and nucleation energy barrier, and consequently suppressed Zn dendrite growth. Galvanostatic cycling of Zn||Zn symmetric cells in different electrolytes at (b) 1 mA cm⁻² and 1 mAh cm⁻², and (c) 5 mA cm⁻² and 5 mAh cm⁻². (d) Coulombic efficiencies of Zn||Cu asymmetric cells. (e) The cycling performance.

redistributes Zn^{2+} ions to the neighboring areas, thereby mitigating the preferential deposition at the tips and promoting a more uniform zinc layer.

Consequently, the cycling stability of Zn plating/stripping was thoroughly assessed using Zn||Zn symmetric cells in different electrolytes. By concurrently regulating the IHP structure and tailoring the surface electric field (Fig. 2a), the symmetric cell employing the EMImOAc/ZnSO₄ electrolyte demonstrated exceptional longevity, sustaining continuous operation for 4200 h at a current density of 1 mA cm⁻² and a capacity of 1 mAh cm⁻² while maintaining a stable overpotential (Fig. 2b). In stark contrast, the cell with the pure ZnSO₄ electrolyte succumbed to a short circuit after a mere 180 h, a failure attributed to dendritic growth that pierced the membrane and sever side reactions (Fig. S5a-d online). When the current density was increased to 5 mA cm⁻², with a corresponding capacity of 5 mAh cm⁻², the cell containing EMImOAc still showcased a remarkable lifespan of over 1480 h. This performance significantly outstripped that of the cell with pure ZnSO₄ electrolyte, which only lasted 90 h (Fig. 2c). Even more impressively, the symmetric cells with the EMImOAc/ZnSO₄ electrolyte maintained robust cycling stability at a range of current densities (Fig. S5e-g online) with a slight increase in hysteresis voltage due to the EMIm⁺ adsorption on the Zn anode surface, outperforming most previous additive-based reports (Fig. S6 online). Additionally, the reversibility of Zn plating/stripping was gauged using Zn||Cu asymmetric cells. The cell containing EMImOAc/ZnSO₄ electrolyte achieved stable cycling for over 1700 cycles (equating to a lifespan of more than 3400 h) at a current density of 1 mA cm⁻², with a high average Coulombic efficiency of 99.40% (Fig. 2d). In contrast, the cell without EMImOAc demonstrated a significantly reduced cycle life of 34 h and an ACE of 94.08%.

The practical applicability of the EMImOAc/ZnSO₄ electrolyte was demonstrated through the synthesis of polyaniline (PANI) to fabricate batteries (Fig. S7 online). The cyclic voltammetry (CV) curves of both ZnSO₄ and EMImOAc/ZnSO₄ electrolytes exhibit similar redox peaks (Fig. S8a online). In contrast, the cell with the EMImOAc/ZnSO₄ electrolyte displays a much narrower peak separation, indicating better redox reversibility due to the presence of EMImOAc (Fig. S8b online). Consequently, within the EMImOAc/ZnSO₄ electrolyte, the cell delivers significantly higher capacities at various current densities compared with the cell with the ZnSO₄ electrolyte (Fig. S8c online). Notably, when the current density is reverted to 0.5 A g⁻¹, the capacity of the cell with EMImOAc/ZnSO₄ electrolyte recovers to 137.4 mAh g⁻¹, confirming the high reversibility of the electrolyte. The long-term cycling performance of Zn||PANI full batteries was also evaluated (Fig. 2e). At a current density of 2 A g⁻¹, the full cell containing the EMImOAc additive exhibits a superior initial capacity of 100.3 mAh g^{-1} and maintains 80.0% of its capacity after 800 cycles, outperforming the cell without the additive, which starts at 91.3 mAh g^{-1} and only retains 51.0% of the capacity (Fig. S8d and e online). Even at a higher current density of 5 A g⁻¹, the full cell with the EMImOAc/ZnSO₄ electrolyte demonstrates a capacity retention of 64.3% after 1500 cycles, significantly better than the 44.5% retention in the ZnSO₄ electrolyte, with the CV results confirming the charge storage process is contributed by both capacitive and diffusion-controlled behaviors (Figs. S8f-i and S9 online).

In summary, we have introduced 1-ethyl-3-methylimidazolium acetate as an innovative additive not only to displace H_2O molecules to form water-depleted IHP, mitigating water decomposition, but also to modulate the electric field at the Zn/electrolyte interface, thereby ameliorating Zn^{2+} ion concentration polarization. Consequently, the zinc anode in an EMImOAc-enhanced electrolyte exhibits remarkable durability, with Zn||PANI full batteries demonstrating commendable capacity retention due to the improved Zn

ion transfer process and suppressed side reactions (Figs. S10–S16 online). Our findings underscore the profound impact of EMImOAc on boosting the stability and reversibility of ZIBs, offering valuable insights for the development of advanced electrolytes applicable to a broad spectrum of battery technologies.

Conflict of interest

The authors declare that they have no conflict of interest.

Acknowledgments

This work was supported by the National Natural Science Foundation of China (22279075) and Shandong Provincial Natural Science Foundation (ZR2020YQ09).

Author contributions

Jian-Jun Wang conceived and supervised the project. Hao Tan, Chao Meng, and Tong Sun designed the experiment and carried out the synthesis and electrochemical measurements. Hong Liu and Xing-Long Wu gave constructive proposals for the manuscript. All the authors discussed the results and commented on the manuscript.

Appendix A. Supplementary materials

Supplementary materials to this short communication can be found online at https://doi.org/10.1016/j.scib.2024.04.061.

References

- Yang XC, Wang XY, Xiang Y, et al. Asymmetric electrolytes design for aqueous multivalent metal ion batteries. Nano-Micro Lett 2024;16:51.
- [2] Sun C, Zhang WD, Qiu DP, et al. Practicable Zn metal batteries enabled by ultrastable ferromagnetic interface. Sci Bull 2023;68:2750–9.
- [3] Liang YL, Yao Y. Designing modern aqueous batteries. Nat Rev Mater 2022;8:109–22.
- [4] Xie XS, Li JJ, Xing ZY, et al. Biocompatible zinc battery with programmable electro-cross-linked electrolyte. Natl Sci Rev 2023;10:nwac281.
- [5] Hao JN, Li XL, Zeng XH, et al. Deeply understanding the Zn anode behaviour and corresponding improvement strategies in different aqueous Zn-based batteries. Energy Environ Sci 2020;13:3917–49.
- [6] Zhang BY, Qin LP, Fang Y, et al. Tuning Zn²⁺ coordination tunnel by hierarchical gel electrolyte for dendrite-free zinc anode. Sci Bull 2022;67:955–62.
- [7] Yu HM, Chen DP, Li QY, et al. *In situ* construction of anode–molecule interface via lone-pair electrons in trace organic molecules additives to achieve stable zinc metal anodes. Adv Energy Mater 2023;13:2300550.
- [8] Sui YM, Ji XL. Electrolyte interphases in aqueous batteries. Angew Chem Int Ed 2024;63:e202312585.
- [9] Yu XY, Li ZG, Wu XH, et al. Ten concerns of Zn metal anode for rechargeable aqueous zinc batteries. Joule 2023;7:1145–75.
- [10] Meng C, He WD, Tan H, et al. A eutectic electrolyte for an ultralong-lived Zn// V₂O₅ cell: An in situ generated gradient solid-electrolyte interphase. Energy Environ Sci 2023;16:3587–99.
- [11] Yan C, Li HR, Chen X, et al. Regulating the inner Helmholtz plane for stable solid electrolyte interphase on lithium metal anodes. J Am Chem Soc 2019;141:9422–9.
- [12] Jiang L, Li DM, Xie X, et al. Electric double layer design for Zn-based batteries. Energy Storage Mater 2023;62:102932.
- [13] Duan GS, Wang Y, Luo B, et al. Taurine-mediated dynamic bridging strategy for highly stable Zn metal anode. Energy Storage Mater 2023;61:102882.
- [14] Luo JR, Xu L, Zhou YJ, et al. Regulating the inner Helmholtz plane with a high donor additive for efficient anode reversibility in aqueous Zn-ion batteries. Angew Chem Int Ed 2023;62:e202302302.
- [15] Xie CL, Liu SF, Wu H, et al. Weak solvent chemistry enables stable aqueous zinc metal batteries over a wide temperature range from -50 to 80 °C. Sci Bull 2023:68:1531-9.
- [16] Peng MK, Tang XN, Xiao K, et al. Polycation-regulated electrolyte and interfacial electric fields for stable zinc metal batteries. Angew Chem Int Ed 2023;62:e202302701.
- [17] Li JW, Zhou S, Chen YN, et al. Self-smoothing deposition behavior enabled by beneficial potential compensating for highly reversible Zn-metal anodes. Adv Funct Mater 2023;33:2307201.



Hao Tan obtained his B.S. degree from Nanjing Tech University, China in 2022. Now, he studies as a master student in Prof. Jian-Jun Wang's group at the State Key Laboratory of Crystal Materials, Shandong University, China. His research interest includes electrolyte design in aqueous Zn-ion batteries.



Hong Liu is a professor at State Key Laboratory of Crystal Materials, Shandong University, and Institute for Advanced Interdisciplinary Research (iAIR), University of Jinan. His current research focuses mainly on photo-electrical functional materials, biosensors, tissue engineering and stem cells, especially the interaction between stem cell and nanostructured biomaterials.



Xing-Long Wu is currently a professor at Northeast Normal University, China. He received his Ph.D. degree from Institute of Chemistry, Chinese Academy of Sciences (ICCAS) in 2011. After continuing a two-year postdoctoral working at ICCAS, he moved to Northeast Normal University as an associate professor in 2013, and became full professor in 2018. His current research interest focuses on the key materials for advanced batteries, and the reuse and recycle of spent batteries.



Jian-Jun Wang is currently a professor at State Key Laboratory of Crystal Materials, Shandong University. He received his Ph.D. degree from ICCAS in 2012 and is mainly engaged in the rational design, synthesis, and applications of novel materials in the fields of artificial photosynthesis and electrochemical energy conversion and storage such as hydrogen production and batteries.